



Stanford
M E D I C I N E

Prediction of Clinical Outcomes in Diffuse Large B-Cell Lymphoma (DLBCL)

Utilizing Radiomic Features

Derived from

Pretreatment Positron Emission
Tomography (PET) Scan

Presenter: Eduardo Somoza Jr M.D, MSc

SCIT Research Fellow

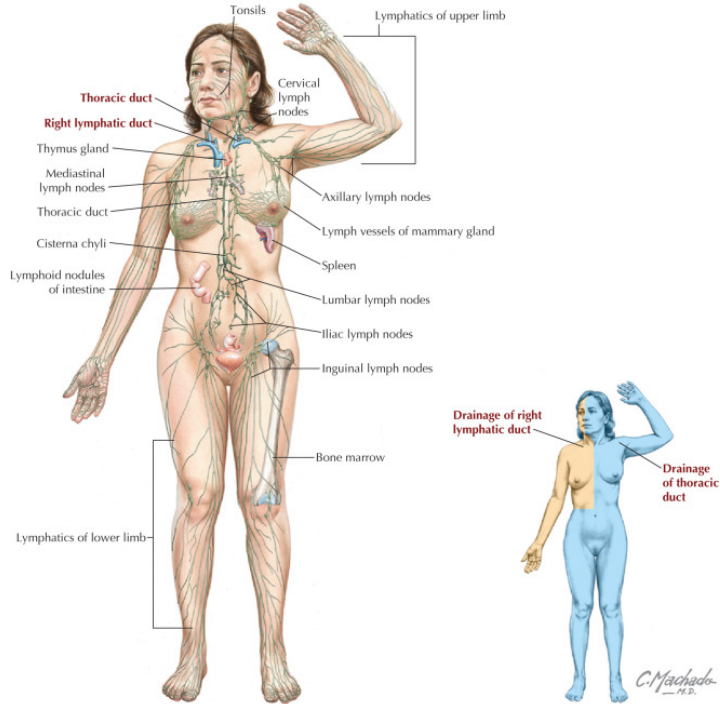
RSL Meeting

January 29th, 2020

Roadmap

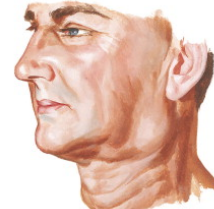
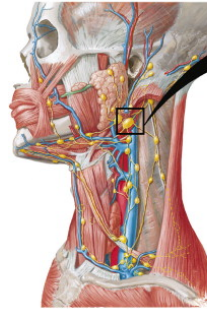
- Background, Clinical Problem, Clinical Need
- Approach
- Projected Phases
- Potential Future Directions

Background: Lymphatic System



Hansen J.T (2018) *Netter' Clinical Anatomy: 4th Edition* Philadelphia, Pennsylvania: Elsevier

▼ Lymph nodes and lymphatic drainage of mouth and pharynx.

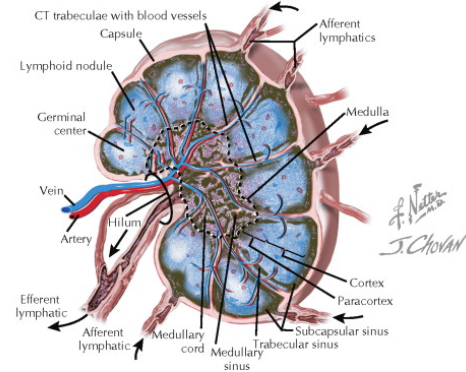


▲ Enlarged cervical lymph node in the neck.
(often first symptom in malignancies of tonsils
fauces, and pharynx)



▲ LM of a lymph node. Surrounded by a capsule (Ca), it has an outer cortex (Co) and central medulla (Me). The hilum is not in the plane of section. The rectangle indicates the area seen at higher magnification in Fig. 9.5. 7x. H&E.

▼ Three-dimensional schematic of a lymph node.



Ovalle WK (2013) *Netter's Essential Histology* Philadelphia, Pennsylvania: Saunders

Background: Lymph Node Histology

Normal Lymph Node Histology

Lymph nodes are part of the lymphatic pathway with connections via afferent and efferent lymphatics. A lymph node is surrounded by a capsule and structurally divided into three areas – cortical, paracortical, and medullary (Fig. 2.1).

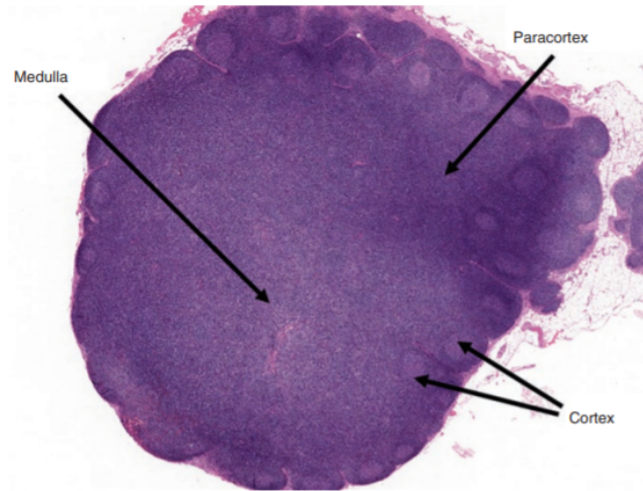


Fig. 2.1 Histology of a normal lymph node showing cortex (B-cell area), paracortex (T-cell area), and medulla

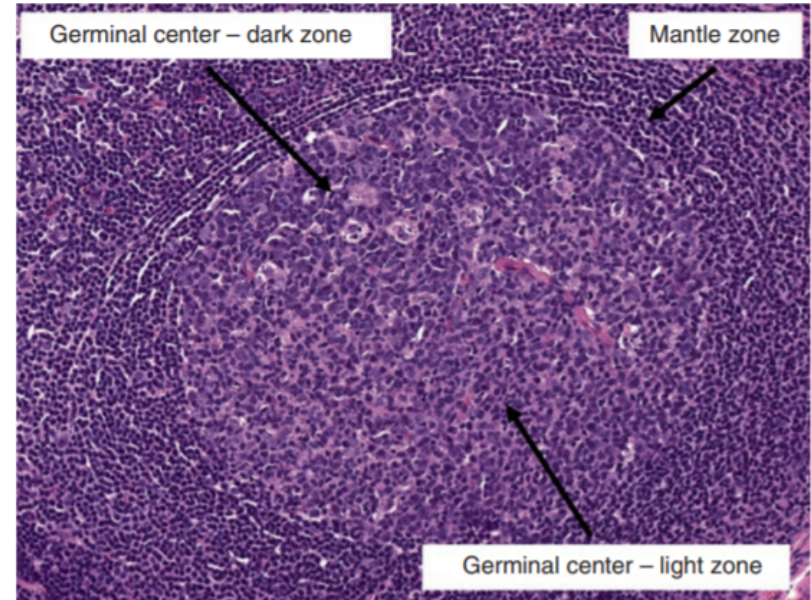


Fig. 2.2 Secondary follicle with germinal center and mantle zone. Marginal zone is not clearly visible in lymph nodes

Background: Lymph Node Histology

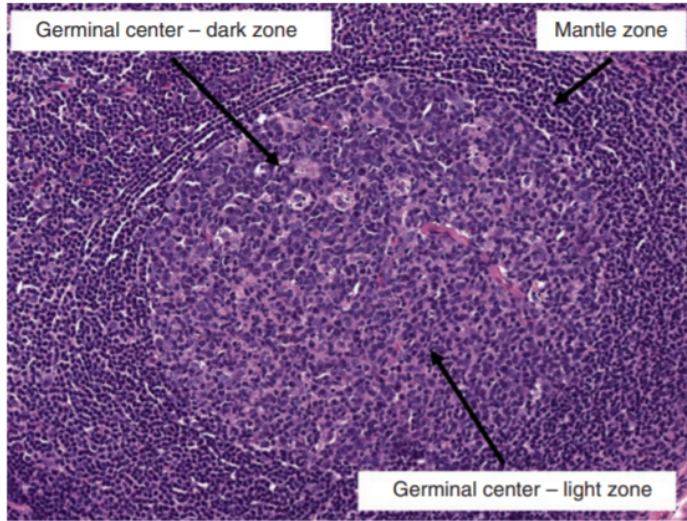


Fig. 2.2 Secondary follicle with germinal center and mantle zone. Marginal zone is not clearly visible in lymph nodes

Normal

Pathology

Involved lymph nodes or tissues show partial or complete effacement of architecture by diffuse infiltration of medium- to large-sized lymphoid cells (Fig. 5.20).

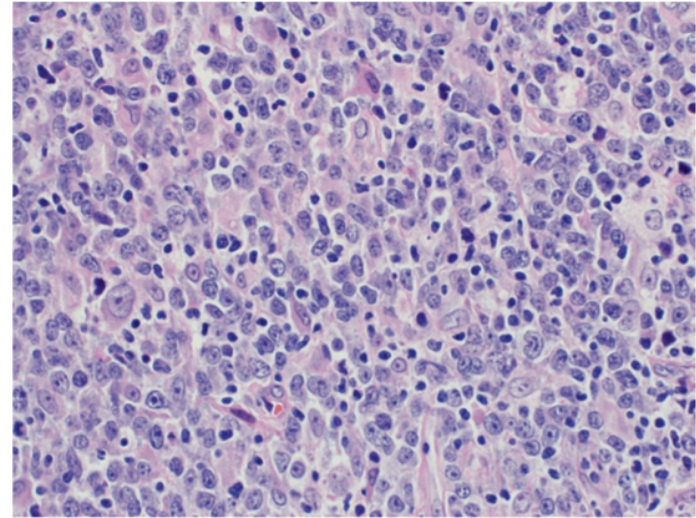


Fig. 5.20 Diffuse large B-cell lymphoma with sheets of large cells with irregular nuclei, open chromatin and one to several prominent nucleoli

Diffuse Large B-Cell Lymphoma (DLBCL)

Clinical Problem: Diffuse Large B-Cell Lymphoma

- Highly aggressive cancer
- Is the most common subtype of Non-Hodgkin's Lymphoma
- Accounts for a quarter of new lymphoma cases
- 30 to 40 percent of patients will relapse after standard treatment¹
- 10 percent will be deemed to have refractory disease¹
- Heterogenous presentation²

Table 1 2016 update of WHO classification of DLBCL: subtypes and related entities

Diffuse large B-cell lymphoma, NOS
GCB versus ABC/non-GCB
MYC and BCL2 double expressor
CD5+
DLBCL subtypes
T-cell/histiocyte-rich large B-cell lymphoma
Primary DLBCL of the central nervous system
Primary cutaneous DLBCL, leg type
EBV positive DLBCL, NOS
Other lymphomas of large B-cells
Primary mediastinal (thymic) large B-cell lymphoma
Intravascular large B-cell lymphoma
DLBCL associated with chronic inflammation
Lymphomatoid granulomatosis
ALK-positive LBCL
Plasmablastic lymphoma
HHV8+ DLBCL, NOS
Primary effusion lymphoma
Borderline cases
High-grade B-cell lymphoma, with <i>MYC</i> and <i>BCL2</i> and/or <i>BCL6</i> translocations
High-grade B-cell lymphoma, NOS
B-cell lymphoma, unclassifiable, with features intermediate between DLBCL and classical Hodgkin lymphoma

ABC, activated B-cell like; DLBCL, diffuse large B-cell lymphoma; GCB, germinal centre B-cell like; HHV8, human herpesvirus 8; NOS, not otherwise specified; WHO, World Health Organization.

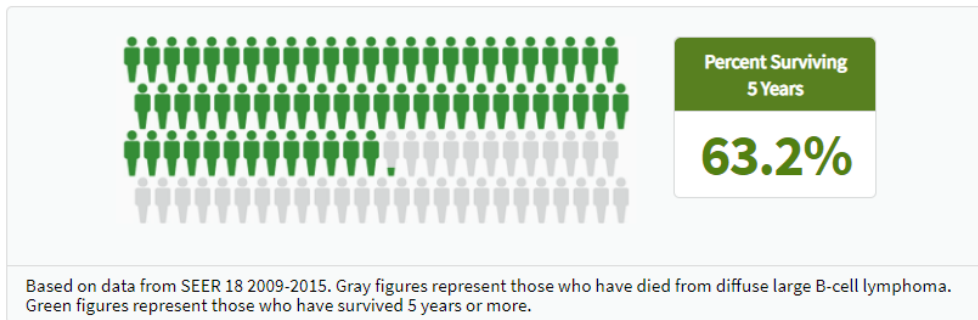
1. Gisselbrecht C et al (2018) *How I manage patients with relapsed/refractory diffuse large B cell lymphoma* British Journal of Haematology 182: 633-643
2. Li S et al (2018) *Diffuse large B-cell lymphoma* Pathology 50 (1): 74-87

Clinical Problem: Survival Statistics

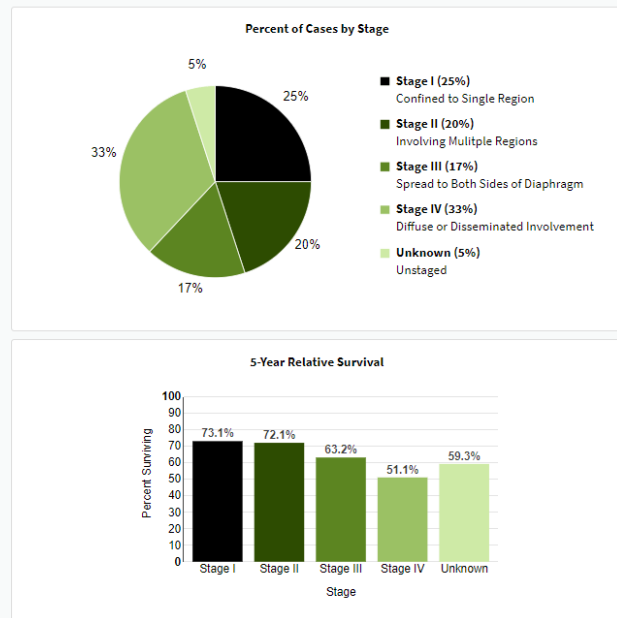
Number of New Cases and Deaths per 100,000: The number of new cases of diffuse large B-cell lymphoma was 5.6 per 100,000 men and women per year. The number of deaths was 1.8 per 100,000 men and women per year. These rates are age-adjusted and based on 2012-2016 cases and deaths.

How Many People Survive 5 Years Or More after Being Diagnosed with Diffuse Large B-Cell Lymphoma?

Relative survival statistics compare the survival of patients diagnosed with cancer with the survival of people in the general population who are the same age, race, and sex and who have not been diagnosed with cancer. Because survival statistics are based on large groups of people, they cannot be used to predict exactly what will happen to an individual patient. No two patients are entirely alike, and treatment and responses to treatment can vary greatly.



Percent of Cases & 5-Year Relative Survival by Stage at Diagnosis: Diffuse Large B-Cell Lymphoma

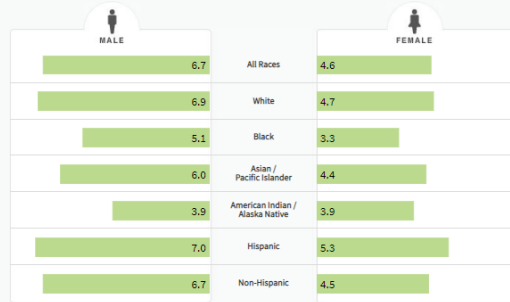


SEER 18 2009-2015, All Races, Both Sexes by Ann Arbor Stage

NIH National Cancer Institute (2019) Cancer Stats Facts: NHL- Diffuse Large B Cell Lymphoma (DLBCL) Retrieved from <https://seer.cancer.gov/statfacts/html/dlbcl.html>

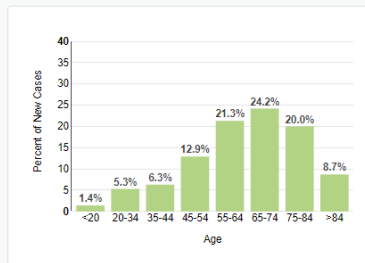
Clinical Problem: Demographics

Number of New Cases per 100,000 Persons by Race/Ethnicity & Sex: Diffuse Large B-Cell Lymphoma (DLBCL)



SEER 21 2012-2016, Age-Adjusted

Percent of New Cases by Age Group: Diffuse Large B-Cell Lymphoma

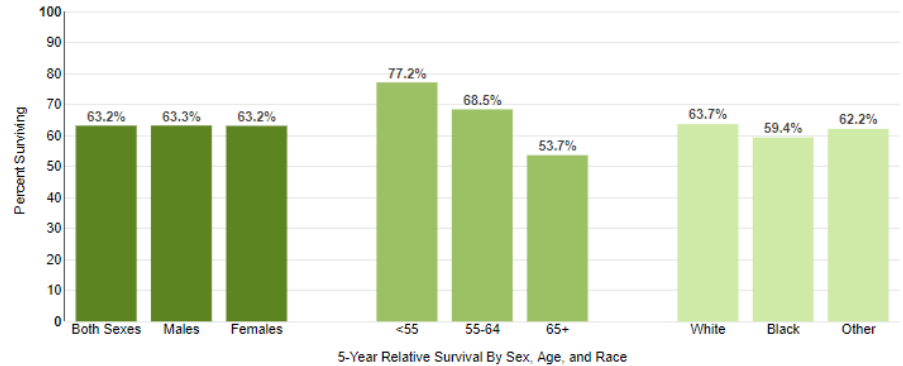


Diffuse large B-cell lymphoma is most frequently diagnosed among people aged 65-74.

Median Age At Diagnosis

66

5-Year Relative Survival by Sex, Age, and Race



SEER 18 2009-2015

Clinical Problem: Treatment & Quality of Life

Treatment ¹	Indication	Effectiveness	Regimen
R-CHOP	Standard Treatment	60 percent Success Rate in Advanced Disease	4-6 Cycles
R-ICE	Salvage Therapy	46 Percent Success Rate	3 Cycles
Allogenic Stem Cell Transplant (ASCT)	Last Option	50 percent will Qualify 50 percent will Relapse	Procedure

Common Side Effects of Chemotherapy

Appetite Constipation Nausea Vomiting	Fatigue Weight Loss Infection Hair Loss	Urinary Changes Mouth Sores Swallowing Chemo Brain	Numbness Pain Sexual Function Fertility
---	--	---	--

Name	Mechanism of Action	Adverse Side Effect
R Rituximab	Monoclonal Antibody	Immune Toxicity
C Cyclophosphamide	DNA Alkylating Agent	Hemorrhagic Cystitis
H Doxorubicin	DNA Intercalation	Cardiotoxicity
O Vincristine	Microtubule Formation	Peripheral Neuropathy
P Prednisone	Glucocorticoid	Immunosuppression

Name	Mechanism of Action	Adverse Side Effect
R Rituximab	Monoclonal Antibody	Immune Toxicity
I Ifosfamide	DNA Alkylating Agent	Hemorrhagic Cystitis
C Carboplatin	DNA Alkylating Agent	Nephrotoxicity
E Etoposide Phosphate	DNA topoisomerase II Inhibitor	Bone Marrow Suppression

1. Gisselbrecht C et al (2018) *How I manage patients with relapsed/refractory diffuse large B cell lymphoma* British Journal of Haematology 182: 633-643

Clinical Problem: Current Prognostic Model

National Comprehensive Cancer Network- International Prognostic Index (NCCN-IPI)^{3,4}

Age

≤40 Years	0
41-60 Years	1
61-75 Years	2
>75 Years	3

Performance Status

ECOG scale:

- 0 - Asymptomatic (Fully active, able to carry on all predisease activities without restriction)
- 1 - Symptomatic but completely ambulatory (Restricted in physically strenuous activity but ambulatory and able to carry out work of a light or sedentary nature. For example, light housework, office work)
- 2 - Symptomatic, <50% in bed during the day (Ambulatory and capable of all self care but unable to carry out any work activities. Up and about more than 50% of waking hours)
- 3 - Symptomatic, >50% in bed, but not bedbound (Capable of only limited self-care, confined to bed or chair 50% or more of waking hours)
- 4 - Bedbound (Completely disabled. Cannot carry on any self-care. Totally confined to bed or chair)

ECOG 0-1	0
ECOG 2-4	1

LDH

Normal	0
Elevated, Up To 3x Upper Limit of Normal	1
>3x Upper Limit of Normal	2

Extranodal Sites

No bone marrow, CNS, liver/GI tract, or lung involvement	0
Bone marrow, CNS, liver/GI tract, or lung involvement	1

Stage

Stage I/II	0
Stage III/IV	1

Overall Score	Prognosis	Percent 5 Year Progression Free Survival	Percent 5 Year Overall Survival
0-1	Low	91	96
2-3	Low-Intermediate	74	82
4-5	High-Intermediate	51	64
≥6	High	30	33

3. Diffuse Large B- cell Lymphoma Prognosis (NCCN-IPI) [2019] Retrieved from https://qxmd.com/calculate/calculator_311/diffuse-large-b-cell-lymphoma-prognosis-nccn-ipi
4. Zhou Z et al (2014) *An enhanced International Prognostic Index (NCCN-IPI) for patients with diffuse large B-cell lymphoma treated in the rituximab era* Blood 124(6): 837-842

Clinical Problem: Issues with NCCN-IPI

- Given that near half of DLBCL patients present with advanced disease (Stage III/IV), a disease specific prognostic model is needed
- Older age and ECOG may be a poor prognostic factors as a result of inability to tolerate chemotherapy
- Lactate Dehydrogenase (LDH) is a non-specific biomarker
- The majority of relapses in DLBCL occur within the first 2 years after completion of standard treatment
- Clinical prognostic models, such as NCCN-IPI, are not built to guide treatment by design

Clinical Need: Versatile Prognostic Model

- The heterogeneity of DLBCL makes it challenging to choose alternative therapies outside of standard treatment
- Due to the high risk of relapse, a “wait and see” treatment approach is problematic in this patient population as it leads to a “trial and error” approach that is detrimental to patient quality of life
- These challenges demonstrate a clinical need for: A versatile prognostic model with the ability to predict clinical outcomes and guide treatment at initial staging of disease

Approach: Positron Emission Tomography (PET)

Examples of PET Capabilities

1. Clinical Diagnosis
2. Clinical Prognosis
3. Treatment Response
4. Verification of Molecular Targets
5. Efficacy of Pharmaceuticals
6. Theranostics

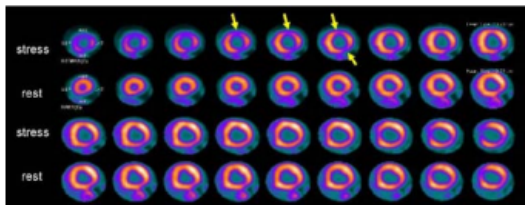


FIGURE 2 PET images of myocardial blood flow during stress and rest in a patient with coronary artery disease. Contiguous tomographic slices of the radiotracer uptake in the myocardium are shown (from left to right). Images in the upper row were obtained during stress and images at the bottom were obtained at rest. Light pink indicates normal and dark blue diminished blood flow. Note the area of reduced blood flow on the stress images (arrows) which is no longer seen on the rest images, indicating the presence of coronary artery disease. SOURCE: Courtesy of Marcelo Di Carli, Harvard University.

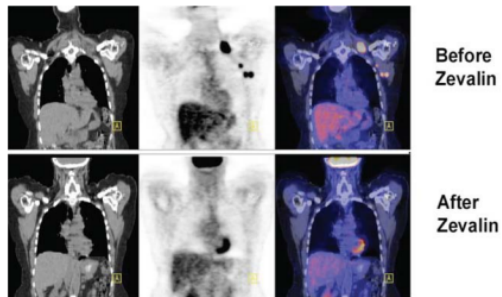


FIGURE 4.5 This set of “before and after” PET/CT images demonstrates the use of these nuclear imaging modalities to evaluate the clinical effects of radioimmunotherapy using radiopharmaceutical compounds such as yttrium-90 ibritumomab tiuxetan (Zevalin®) in the treatment of malignant lymphoma. SOURCE: Courtesy of Peter Conti, University of Southern California.

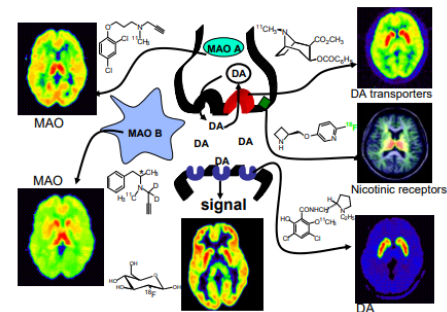


FIGURE 6.2 Radiotracers for imaging neurotransmitter function, as exemplified in the brain dopamine system. A simplified diagram of a dopamine (DA) synapse shows the dopamine transporter (red), dopamine receptors (blue), and monoamine oxidase (MAO) A and B, a nicotine binding site (green), and brain glucose metabolism along with radiotracer structures and human brain images corresponding to each of these molecular targets. SOURCE: Courtesy of Joanna Fowler, Brookhaven National Laboratory.

Positron Emission Tomography (PET): Principle

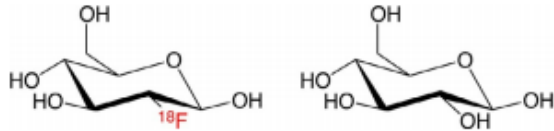


Fig. 11.3. The chemical structure of ^{18}F -fluorodeoxyglucose (FDG) (left) is very similar to glucose (right); in FDG the 2' hydroxyl group has been replaced by ^{18}F .

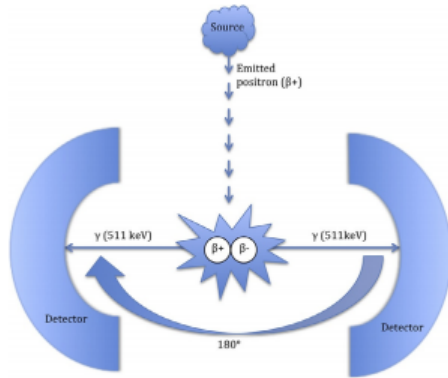


Fig. 11.1. After being emitted, positrons travel a distance before combining with an electron in an annihilation event. This results in the production of two antiparallel 511 keV photons which strike opposing detectors within a coincidence time window.

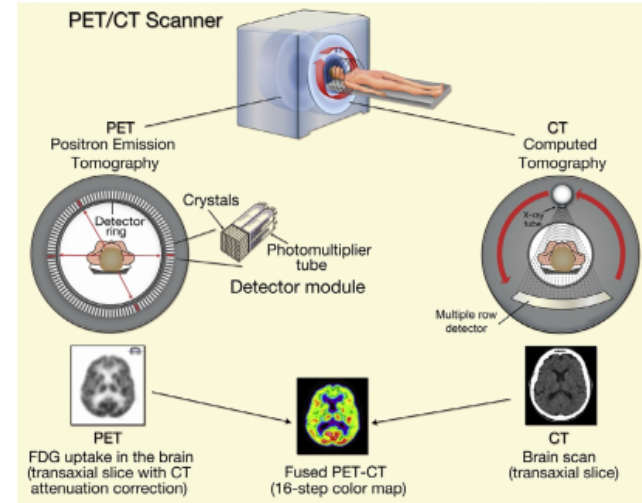


Fig. 11.4. Typical multimodality positron emission tomography (PET)/computed tomography (CT) imaging system combining a state-of-the-art PET scanner, for molecular imaging, with a multiple-detector-row CT scanner, for anatomic imaging. The software and hardware are optimized to acquire complementary information from a patient bed moving through both scanners. For the CT component of the scan, lasting seconds, the table moves uninterrupted while a continuous volume is acquired in spiral scan mode. For PET images, the bed moves in incremental steps based on the PET detectors' field-of-view (typically 16.2 cm) with each acquisition typically taking 3–6 minutes. The PET detector ring is shown with a multicrystal scintillation detector and photomultiplier tubes. The electronics and detector localize annihilation-photon absorption to a single crystal. FDG, ^{18}F -fluorodeoxyglucose. (Reproduced with permission from Esser, 2009.)

Positron Emission Tomography (PET): Workflow

Pretreatment

Acquired before
initiation of standard
treatment

Baseline PET used for:

Risk stratification

NCCN-IPI using PET discriminates patients with very good prognosis from patients at high risk of treatment failure, mostly elderly patients unsuitable for salvage treatments for whom testing with novel agents may be appropriate
Parameters including number of extranodal sites and metabolic tumour burden, also combined with early response are promising predictors of prognosis.

Staging including bone marrow assessment

Can replace bone marrow biopsy in selected cases

Mapping initial disease sites for accurate response assessment

Differentiating lymphomatous involvement from other causes for increased FDG uptake, e.g. infection, inflammation, bone marrow hyperplasia

Response

Acquired 2- 4 cycles
into standard
treatment

Interim PET used for:

Prognosis

Early CMR has excellent prognosis and usually predicts CMR at end of treatment; such patients do not require end-of-treatment scans.

Patients with a positive interim PET and other high risk features, e.g. poor-risk IPI, may require close monitoring during treatment as they have higher risk of refractory disease and relapse.

PET is a more appropriate test for interim imaging assessment than CT.

Excluding disease progression on treatment

But should not be used to change standard treatment unless clear evidence of progression. To date, no evidence exists that response adaptation at interim on the basis of positive PET improves patient outcomes and risks over-treating many patients.

Post treatment

Acquired up to 8
weeks after last cycle
of standard
treatment

End of treatment PET used for:

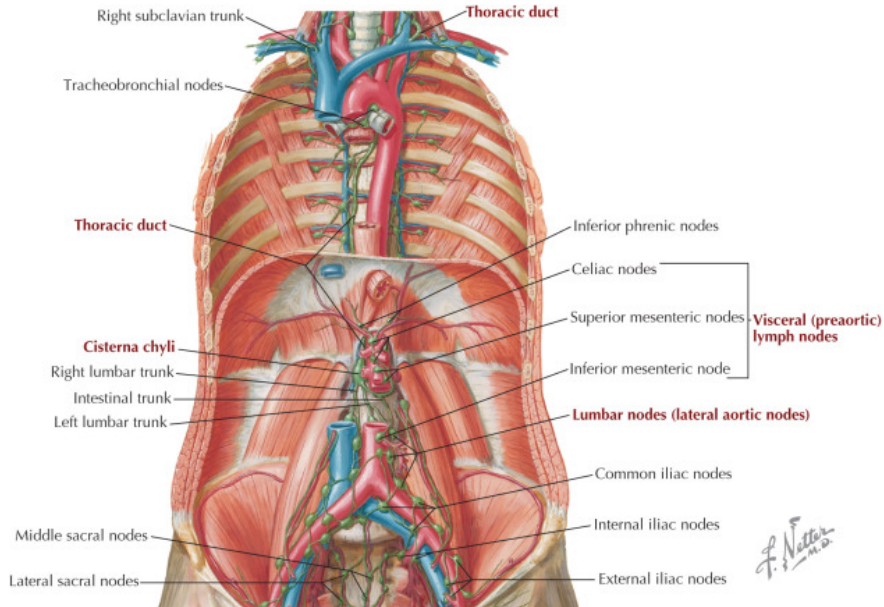
Remission assessment

Using Deauville criteria. Patients with end-of-treatment Deauville scores 4 and 5 should be considered for further treatment with biopsy confirmation wherever feasible but particularly if salvage treatment ± ASCT is being considered.

Decision making as to suitability for ASCT following high-dose chemotherapy
In preference to CT



Positron Emission Tomography (PET): DLBCL Example



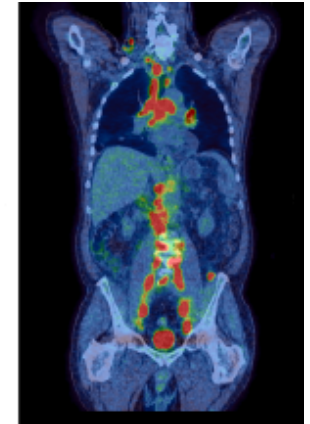
CT Scan
Structural



PET Scan
Functional



Fusion
Image



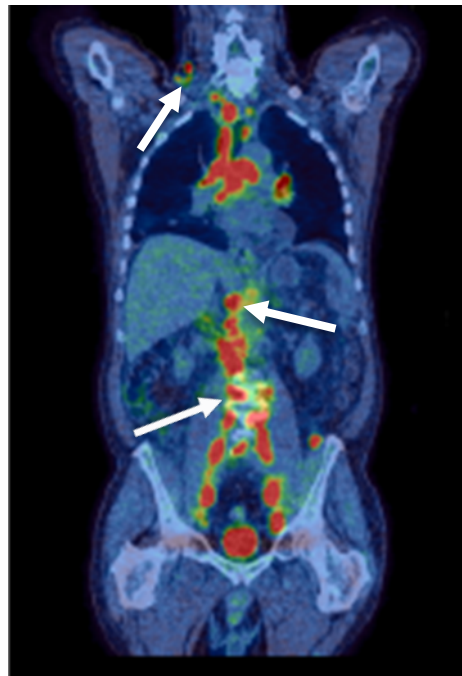
Example of Stage IV DLBCL⁵

Hansen J.T (2018) *Netter' Clinical Anatomy: 4th Edition* Philadelphia, Pennsylvania: Elsevier

5. Barrington S.F et al (2016) *PET Scans for Staging and Restaging in Diffuse Large B-Cell and Follicular Lymphomas* Current Hematologic Malignancy Reports 11: 185-195

Current Approach: Lymph Node Biopsy with PET

- PET imaging is used to select a lymph node for biopsy
- Lymph node biopsy is taken to confirm disease
- Sometimes biopsy is not feasible to obtain
- Regardless, a single biopsy does not reflect the heterogeneity of disease
- This is an issue when molecular analysis can impact treatment
- As the pretreatment PET scan is a functional imaging modality, thus providing physiological information of disease, can we select multiple lymph nodes to reflect the heterogeneity of DLBCL for individual patients?



5. Barrington S.F et al (2016) *PET Scans for Staging and Restaging in Diffuse Large B-Cell and Follicular Lymphomas* Current Hematologic Malignancy Reports 11: 185-195

Current Approach: Selection of Nodes with PERCIST

- PERCIST: Positron Emission Tomography (PET) Response Criteria in Solid Tumors⁶

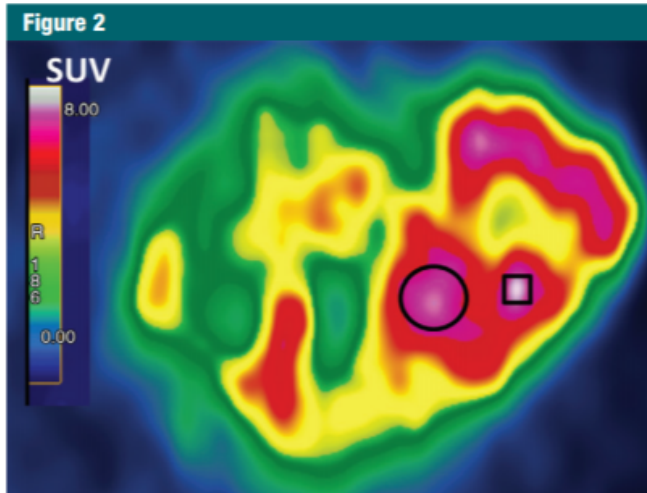


Figure 2: Magnified transverse FDG PET image shows a single large heterogeneous tumor. SUL_{peak} was the mean from a three-dimensional 1-mL sphere approximately 1.2 cm in diameter in tumor area, yielding highest average SUL (represented here as circle instead of sphere). SUL_{peak} does not necessarily contain maximum standardized uptake value (SUV, square), which is the highest single pixel value.

Table 2

Recommended Exploratory Data to Consider for Collection

Variable and Consideration

SUL_{peak} of up to the five hottest tumors
Mean SUL in 1-mL spherical VOIs is calculated.
Five hottest assessable SUL_{peak} values at baseline are included.
Up to two lesions per organ are evaluated.
To calculate percentage of change in SUL of five lesions, data from each lesion is summed before and after treatment.*
Maximum SUL
Mean SUL at 50% and 70% of SUL_{peak} or maximum SUL
PET-derived metabolic tumor volume [†]
>50% of SUL_{peak}
>mean SUL + 2SD of liver
>mean SUL + 3SD of liver
>1.5 · mean SUL + 2SD of liver
Liver mean SUL and SD from 3-cm spherical VOI: for all tumor foci, five lesions with highest SUL, or one lesion with highest SUL
Total lesion glycolysis [‡]
Total lesion glycolysis = mean SUL of total tumor times total metabolic tumor volume in milliliters
Total lesion glycolysis increase \geq 75% categorized as progressive metabolic disease
Total lesion glycolysis decrease \geq 45% categorized as partial metabolic response
Nonassessable tumors
Tumors with FDG uptake < 1.5 · (mean SUL) + 2SD
Note and measure disappearance, or obvious progression, segregating the data
Tumor sizes according to Response Evaluation Criteria in Solid Tumors 1.1

Note.—SD = standard deviation.

* Change in data required for categorization as partial metabolic response and progressive metabolic disease with more than one target lesion is yet undefined.

[†] FDG uptake of tumor lower than the threshold for metabolic tumor volume could be zero at follow-up, even when SUL_{peak} does not show complete metabolic response.

[‡] Threshold percentage for response assessment of total lesion glycolysis is undefined.

Alternative Approach: Radiomic Biopsy

- Definition: Radiomics is predicated on the beliefs that these images reflect underlying pathophysiologies, and that they can be converted into mineable data for improved diagnosis, prognosis, prediction, and therapy monitoring⁷.

Radiomic Features
<p>14 first order statistics: Energy, entropy, kurtosis, maximum, mean, mean absolute deviation, median, minimum, range, root mean square, skewness, standard deviation (Std), uniformity, variance.</p>
<p>8 shape- and size-based features: Compactness 1, compactness 2, maximum 3D diameter, spherical disproportion, sphericity, surface area, surface to volume ratio, volume.</p>
<p>34 textural features: Autocorrelation, cluster prominence, cluster shade, cluster tendency, contrast, correlation, difference entropy, dissimilarity, difference variance, energy_c, entropy_c, homogeneity 1, homogeneity 2, informational measure of correlation 1 (IMC1), informational measure of correlation 2 (IMC2), inverse difference moment normalized (IDMN), inverse difference normalized (IDN), inverse variance, maximum probability, sum average, sum entropy, sum variance, variance, short run emphasis (SRE), long run emphasis (LRE), gray-level non-uniformity (GLN), run length non-uniformity (RLN), run percentage (RP), low gray-level run emphasis (LGLRE), high gray-level run emphasis (HGLRE), short run low gray-level emphasis (SRLGLE), short run high gray-level emphasis (SRHGLE), long run low gray-level emphasis (LRLGLE), long run high gray-level emphasis (LRHGLE).</p>
<p>384 wavelet features: Wavelet features consist of the first order statistics and textural features extracted from eight wavelet decompositions (X_{HHH}, X_{HHL}, X_{HLH}, X_{HLL}, X_{LHH}, X_{LHL}, X_{LLH}, and X_{LLL}). For example, Energy_HHL represents the energy feature calculated from decomposition X_{HHL}.</p>

Table 1. The detailed radiomic features.

Example of Radiomic Features⁸

7. Napel S et al (2018) *Quantitative imaging of cancer in the postgenomic era: Radio (geno) mics, deep learning, and habitats* Cancer 124(24): 4633-4649

8. Xiong J et al (2018) *The Role of PET-Based Radiomic Features in Predicting Local Control of Esophageal Cancer treated with Concurrent Chemoradiotherapy* Scientific Reports 8: 9902

Prognostic Model: Feature Extraction

- The Quantitative Image Feature Pipeline (QIFP) will be utilized⁹
- Input for model will be radiomic features derived from pretreatment PET Scan
- Output will be a linear model
- Clinical Outcome to be predicted will be Binary
- Example: 2-year Progression Free Survival was achieved or not

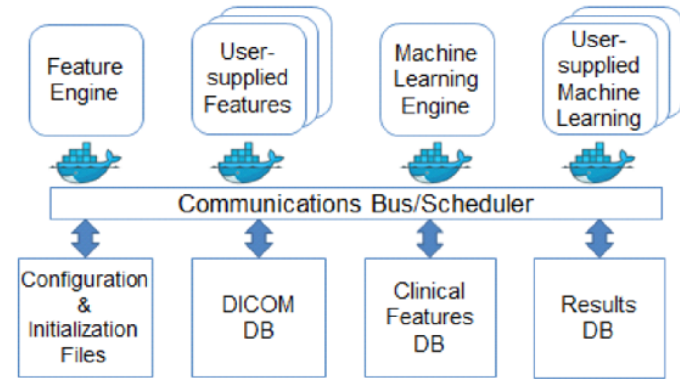


Fig. 1 QIFP architecture. The top half of the figure represents a Docker image capable of given task, such as feature extraction or machine learning. The lower half shows the connections to run configuration options files and to various local databases, such as Dicom images/segmentations, clinical features, or workflow results.

9. Mattonen SA et al (2020) *Quantitative Imaging Feature Pipeline (QIFP): A web-based tool for utilizing, sharing, and building image processing pipelines SPIE: Journal of Medical Imaging*, Accepted Pending Revisions

Prognostic Model: Stratification

- The clinical outcome is 2-Year Progression Free Survival (2-yr PFS)
- The prognostic model will be able to group patients based on whether or not they achieve 2-yr PFS
- Will compare the molecular pathology, clinical prognostic scores, demographics, and risk factors between the two subgroups
- Will allow for the isolation of non-imaging attributes that can possibly guide treatment

Molecular Marker of DLBCL²

Markers	Frequency	Significance
CD19	Often	Diagnosis, target
CD20	Often	Diagnosis, target
CD22	Often	Diagnosis, target
CD79a/CD79b	Often	Diagnosis
PAX5	Often	Diagnosis
sIg or cytoIg	50–75%, IgM more common	Diagnosis
CD5	5–10%	Prognosis
CD30	Variably expressed, more in anaplastic	Prognosis, target
CD10	30–60%	All 3 markers (CD10, BCL6, MUM1) combined to define GCB vs non-GCB
BCL6	60–90%	
MUM1	35–65%	
Ki67	Variably expressed in every case, usually >40%	Proliferative marker
MYC	20–40%	Coexpression define Prognosis, target
BCL2	Often	
P53	Variable depending on cut-off	

DLBCL, diffuse large B-cell lymphoma.

2. Li S et al (2018) *Diffuse large B-cell lymphoma* Pathology 50 (1): 74-87

Projected Phases

Nov 2019	Dec 2019	Jan 2020	Feb 2020	Mar 2020	Apr 2020	May 2020	June 2020
-------------	-------------	-------------	-------------	-------------	-------------	-------------	--------------

3-4 mos

1-2 mos

1-2 mos

1 mo

1 mo

1. Creation of Clinical Database
2. Creation of Imaging Database
3. Clinical Image Analysis
4. Generation of Prognostic Model
5. Incorporation of Clinical Data

Potential Future Directions

- Evaluation of prognostic model to guide initial treatment
- Incorporation of pathology into prognostic model
- Measure clinic value of radiomic biopsy
- Correlation between radiomic biopsy and cell free DNA
- Comparison to a Deep Learning Approach

Acknowledgements

SCIT Program

About

Organization

Courses

Resources

Diversity

Alumni

Leadership

Mentors & Research

Trainees

Seminars

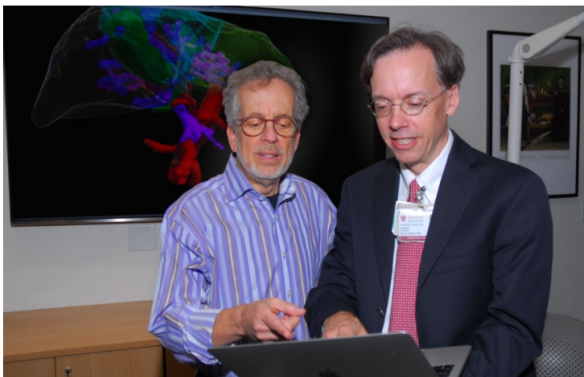
Apply

Contact Us

SCIT Program



About the SCIT Program



The Stanford Cancer Imaging Training (SCIT) Program, funded by the [National Cancer Institute](#), aims to train the next generation of researchers in the development and clinical application of advanced techniques for cancer imaging. Our coursework, rich mentored training opportunities, and outstanding resources, provide an active, vibrant program that attracts students nationwide. Graduates from our program are highly sought after, filling faculty and industry research positions internationally. This two-year Training Program accepts only US citizens or permanent residents and will help develop a US workforce to make progress in the battle against cancer.

Led by Program Directors [Sandy Napel, PhD](#), and [Bruce Daniel, MD](#), the objectives of the SCIT program are to:

Recruit and to train the next generation of cancer-imaging scientists, equipping them with critical technical and

Guido Davidzon



Guido Davidzon

Radiologist



Clinical Assistant Professor, Radiology - Rad/Nuclear Medicine

Dr. Guido A. Davidzon is a physician-scientist board certified in Nuclear Medicine. He is an attending physician in Nuclear Medicine and Molecular Imaging at Stanford Health Care.



Sandy Napel

PROFESSOR OF RADIOLOGY (INTEGRATIVE BIOMEDICAL IMAGING INFORMATICS) AND, BY COURTESY, OF MEDICINE (MEDICAL INFORMATICS) AND OF ELECTRICAL ENGINEERING

Web page: <http://web.stanford.edu/people/Sandy.Napel>

References

1. Gisselbrecht C et al (2018) *How I manage patients with relapsed/refractory diffuse large B cell lymphoma* British Journal of Haematology 182: 633-643
2. Li S et al (2018) *Diffuse large B-cell lymphoma* Pathology 50 (1): 74-87
3. Diffuse Large B- cell Lymphoma Prognosis (NCCN-IPI) [2019] Retrieved from https://qxmd.com/calculate/calculator_311/diffuse-large-b-cell-lymphoma-prognosis-nccn-ipi
4. Zhou Z et al (2014) *An enhanced International Prognostic Index (NCCN-IPI) for patients with diffuse large B-cell lymphoma treated in the rituximab era* Blood 124(6): 837-842
5. Barrington S.F et al (2016) *PET Scans for Staging and Restaging in Diffuse Large B-Cell and Follicular Lymphomas* Current Hematologic Malignancy Reports 11: 185-195
6. O et al (2016) *Practical PERCIST: A Simplified Guide to PET Response Criteria in Solid Tumors 1.0* Radiology, 280: 576-584
7. Napel S et al (2018) *Quantitative imaging of cancer in the postgenomic era: Radio (geno) mics, deep learning, and habitats* Cancer 124(24): 4633-4649
8. Xiong J et al (2018) *The Role of PET-Based Radiomic Features in Predicting Local Control of Esophageal Cancer treated with Concurrent Chemoradiotherapy* Scientific Reports 8: 9902
9. Mattonen SA et al (2020) *Quantitative Imaging Feature Pipeline (QIFP): A web-based tool for utilizing, sharing, and building image processing pipelines* SPIE: Journal of Medical Imaging, Accepted Pending Revisions